Published in final edited form as:

Addict Biol. 2016 July ; 21(4): 972–981. doi:10.1111/adb.12262.

Lower grey matter density and functional connectivity in the anterior insula in smokers compared to never-smokers

Luke E. Stoeckel[1,2,*], **Xiaoqian J. Chai**[3,*], **Jiahe Zhang**[3], **Susan Whitfield-Gabrieli**[3,#], and **A. Eden Evins**[1,2,#]

[1]Massachusetts General Hospital, Department of Psychiatry

[2]Harvard Medical School

[3]Department of Brain and Cognitive Sciences, Poitras Center for Affective Disorders Research, McGovern Institute for Brain Research, Massachusetts Institute of Technology

Abstract

Rationale—While nicotine addiction is characterized by both structural and functional abnormalities in brain networks involved in salience and cognitive control, few studies have integrated these data to understand how these abnormalities may support addiction.

Objectives—(1) To evaluate grey matter density and functional connectivity of the anterior insula in cigarette smokers and never-smokers and (2) characterize how differences in these measures related to smoking behavior.

Methods—We compared structural MRI (grey matter density via voxel-based morphometry) and seed-based functional connectivity MRI data in 16 minimally deprived smokers and 16 matched never-smokers.

Results—Compared to controls, smokers had lower grey matter density in left anterior insula extending into inferior frontal and temporal cortex. Grey matter density in this region was inversely correlated with cigarettes smoked per day. Smokers exhibited negative functional connectivity (anti-correlation) between the anterior insula and regions involved in cognitive control (left lateral prefrontal cortex) and semantic processing / emotion regulation (lateral temporal cortex), whereas controls exhibited positive connectivity between these regions.

Conclusions—There were differences in the anterior insula, a central region in the brain's salience network, when comparing both volumetric and functional connectivity data between

Address correspondence to: Luke E. Stoeckel, PhD, Massachusetts General Hospital Center for Addiction Medicine, 60 Staniford Street, Boston, MA 02114 USA, lstoeckel@mgh.harvard.edu Fax: 617-643-1998.

*,#These authors contributed equally to the work.

Author Contributions

LES, XJC, SWG and AEE were responsible for the study concept and design. LES and XJC were responsible for data collection. LES, XJC, JZ performed the data analysis. LES drafted the manuscript. XJC, JZ, SWG, and AEE provided critical revision of the manuscript for important intellectual content. All authors critically reviewed content and approved final version for publication.

Conflicts of Interest

The authors report no conflicts of interest.

Financial Disclosures

There are no additional disclosures to report.

cigarette smokers and never smokers. Volumetric data, but not the functional connectivity data, was also associated with an aspect of smoking behavior (daily cigarettes smoked).

Keywords

salience; executive function; nicotine addiction; functional connectivity; voxel-based morphometry

Introduction

Dysfunction in brain systems mediating salience is critical for the development of addictions, including nicotine addiction. The anterior insula is the primary node of the salience network (Menon and Uddin, 2010; Seeley et al., 2007). The salience network interfaces with cognitive control neurocircuitry, including lateral prefrontal cortex (PFC), to control interpretation of internal biological and external environmental cues, including emotional responses and associated goal-directed behaviors (Buhle et al., 2013; Kalivas and Volkow, 2005; Whitney et al., 2011). Abnormalities have been reported in both the structure and functional architecture of cigarette smoker's brains in these areas, even when at rest and not engaged in goal-directed behavior (Brody et al., 2004; Clewett et al., 2014; Gallinat et al., 2006; Janes et al., 2012; Kuhn et al., 2012; Lerman et al., 2014; Morales et al., 2014; Sutherland et al., 2013a; Sutherland et al., 2013b; Sutherland et al., 2012; Zhang et al., 2011a; Zhang et al., 2011b).

Previous structural (volumetric, diffusion-tensor imaging) and functional connectivity MRI studies have found abnormalities in several other brain regions and networks, in addition to anterior insula and lateral PFC, implicated in nicotine addiction, including, but not limited to, brain stem structures (e.g., ventral tegmental area), thalamus, striatum, areas of cortex (e.g., ventromedial PFC, anterior cingulate cortex), and cerebellum (see Goriounova and Mansvelder, 2012; Pan et al., 2013; Schuman-Olivier et al., 2014; Sutherland et al., 2012 for recent a meta-analysis and reviews). These different brain regions and networks have been shown to relate to different aspects of smoking behavior, most commonly lifetime exposure to nicotine and severity of nicotine dependence. However, there is considerable variability across studies, both in the brain regions and networks that differentiate smokers from non-smokers and in the brain-smoking behavior relationships observed within smokers (see Franklin et al., 2014 and Sutherland et al., 2012 for further discussion of this issue).

Most human functional connectivity magnetic resonance imaging (MRI) studies in tobacco smokers have focused on effects within the default mode network and its interactions with other regions/networks, e.g., (Cole et al., 2010), with 4.5 – 24 hours of abstinence, when withdrawal symptoms may influence brain function, e.g., (Hong et al., 2009; Lerman et al., 2014; Sutherland et al., 2013b), or using data-driven analytic approaches (e.g., Independent Component Analysis) to explore large-scale network properties that do not provide the spatial localization of hypothesis-driven seed-based functional connectivity analysis, e.g., (Breckel et al., 2013; Janes et al., 2014). Only one published multimodal neuroimaging study to date compared combined structural (voxel-based morphometry and diffusion-tensor imaging) and resting state fMRI in smokers and non-smokers (Zhang et al., 2011b). In this study, there were differences in several PFC brain networks that correlated with smoking

cue-induced brain function; however, there was convergence on one particular region, dorsolateral PFC, which emerged when combining both the structural and functional data (Zhang et al., 2011b). This highlights one potentially important role for multi-modal neuroimaging studies: structural data can be used to inform which brain region(s) to select as seed regions for brain activation and connectivity studies that can address questions about function and the relationship to processes of relevance to addiction.

In this study, we collected structural and resting state functional MRI data to investigate differences in brain structure (grey matter density, using voxel-based morphometry or VBM) and functional connectivity (using a region-of-interest, seed-based approach) in never-smokers and minimally-deprived (~1 hour abstinent) cigarette smokers. We correlated these brain measures with smoking behavior (lifetime exposure to nicotine and severity of nicotine dependence) in cigarette smokers. We used an exploratory, whole-brain approach to identify regional clusters in the structural MRI data where there were group differences between smokers and never-smokers to guide selection of regions of interest (ROIs) for the functional connectivity analyses (see the Materials and Methods section for further details). We expected to find differences in brain structure and functional connectivity between smokers and never-smokers in networks, like the salience network, that may underlie the high motivational potency and salience of nicotine and control of smoking behavior through this mechanism.

Materials and Methods

Participants

Thirty-two participants (16 non-deprived, non-treatment-seeking cigarette smokers and 16 never-smoking control participants) were included in the study (see Table 1 for participant characteristics). Data for control participants was selected from healthy controls from an existing dataset (Doehrmann et al., 2013). Participants were selected for inclusion in the study such that there were no group differences in age, gender, or education (all *ps* > .1). Participants in the never-smoking, control group responded ‘no’ to the question: ‘Have you ever smoked cigarettes?’. Data collection occurred on the same MRI machine during a similar time period for both groups and the protocols for MRI data acquisition and analysis were identical. Eligible participants were aged 18–55 years, right-handed, and had normal or corrected-to-normal visual acuity. Exclusion criteria included inability to speak or understand the English language; being pregnant; serious unstable medical illness; cerebrovascular or cardiovascular illness; lifetime history of psychiatric disorder, developmental disability, or substance use disorder other than nicotine or caffeine in the past 12 months per Structured Clinical Interview for the DSM-IV (SCID) (First, 2007). Smokers were enrolled if they reported smoking an average of ≥10 cigarettes/ day for at least the past 6 months and had expired CO >10 ppm at screening, reported no smoking cessation plan within the next 30 days, and had normal affect by self report (positive affect > 12.5 and negative affect < 29.1) on the Positive and Negative Affect Scale; PANAS (Watson et al., 1988). Participants were recruited via online advertisements and flyers in the greater Boston area and provided written informed consent prior to study procedures, which were approved by the Massachusetts General Hospital and Massachusetts Institute of Technology

institutional review boards in accordance with the ethical standards established by the 1964 Declaration of Helsinki.

Imaging procedures

Scanning procedures were conducted at the Martinos Imaging Center at the Massachusetts Institute of Technology. Scanning began approximately 1 hour after participants arrived at the center. Upon arrival, participants in the smoking group were monitored while they smoked a cigarette prior to beginning study activity to standardize the time since last cigarette. Data were acquired on a 3T TrioTim Siemens scanner using a 32-channel head coil. First, T1-weighted whole brain anatomical images (MPRAGE sequence, 256×256 voxels, 1×1.3-mm in-plane resolution, 1.3-mm slice thickness) were collected. Participants then underwent a resting functional MRI scan of 6.2 min with the instructions “relax and keep your eyes open and fixated on the crosshair”. Resting images were obtained in 67 2-mm thick transverse slices, covering the entire brain (interleaved EPI sequence, T2*-weighted images; repetition time = 6 s, echo time = 30 ms, flip angle = 90, 67 slices with 2×2×2 mm voxels). Online prospective acquisition correction (PACE) was applied to the EPI sequence.

Voxel-based morphometry analysis

Voxel-based morphometry (VBM) analysis was performed using the default approach implemented in the VBM8 toolbox (http://dbm.neuro.uni-jena.de/vbm/) within SPM8 (http://www.fil.ion.ucl.ac.uk/spm/) running on MATLAB R2010b (Mathworks). The VBM8 toolbox steps include bias correction, tissue classification and affine registration. The affine registered grey matter (GM) and white matter (WM) segmentations were used to build a customized DARTEL (diffeomorphic anatomical registration through exponentiated lie algebra) template (Ashburner, 2007). Then warped GM and WM segments were created. Modulation was applied in order to preserve the volume of a particular tissue within a voxel by multiplying voxel values in the segmented images by the Jacobian determinants derived from the spatial normalization step. Finally, images were smoothed with a full-width half-maximum kernel of 8 mm. Whole-brain, independent-samples t-tests were used to compare GM density between smokers and non-smokers. The resulting maps were thresholded using a height threshold of $p < .001$, and an extent threshold of FWE-corrected $p < 0.05$) combined with a nonstationary smoothness correction (cluster extent = 768; (Hayasaka and Nichols, 2004)).

fMRI data preprocessing

Functional data were slice-time corrected, realigned and resliced, and smoothed with a 6-mm kernel in SPM8 (Wellcome Department of Imaging Neuroscience, London, UK; http://www.fil.ion.ucl.ac.uk/spm). *Normalization*: cortical reconstruction and parcellation of the anatomical images was performed with FreeSurfer, v5.1.0 (Dale et al., 1999), the accuracy of which was verified manually via visual inspection. FreeSurfer and FSL, v5.0 (http://fsl.fmrib.ox.ac.uk/fsl/fslwiki/) were used to coregister participants’ mean functional and high-resolution anatomical images. These tools were also used to create an anatomical mask consisting of intracranial voxels only for subsequent fMRI analyses. The functional and structural data were then normalized to MNI space using Advanced Normalization Tools

(ANTS) v.1.9.y (Avants et al., 2009). First, a custom group template was created from each subject's structural image. Next, the custom group template was normalized to the MNI152 1 mm T1 template from FSL (Smith et al., 2004). Finally, the functional data were warped to the custom group template in MNI space (for normalization details, see (Perrachione and Ghosh, 2013)). This approach to normalization led to superior registration results (i.e., better localization of function and larger effects sizes) when compared to a standard normalization routine in SPM8 on an independent dataset (data not shown).

Head motion and artifact detection

Participant head motion, as measured by the mean translation in x, y, z directions, did not differ between smokers (mean = .24mm ± .11) and controls (mean = .23mm ± .16; p = .814). To address the spurious correlations in resting-state networks caused by head motion across participants, we identified problematic time points during the scan using Artifact Detection Tools (ART, http://www.nitrc.org/projects/artifact_detect/). Specifically, an image was defined as an outlier (artifact) image if the head displacement in x, y, or z direction was greater than .5mm from the previous frame, or if the rotational displacement was greater than .02 radians from the previous frame, or if the global mean intensity in the image was greater than 3 standard deviations from the mean image intensity for the entire resting scan. The number of outlier images did not differ between smokers (mean = 1.00 ± 1.75) and controls (mean = 1.44 ± 3.14; p = .630). Outlier images were modeled in the first level general linear model (GLM). Each outlier was represented by a single regressor in the GLM, with a 1 for the outlier time point and 0 elsewhere.

Functional connectivity analysis

Functional connectivity analysis was performed using a seed-driven approach with in-house, custom software "CONN" (Chai et al., 2012; Whitfield-Gabrieli and Nieto-Castanon, 2012). We created an ROI mask in SPM8 from the grey matter cluster primarily in left anterior insula extending into inferior frontal and lateral temporal cortices that differentiated smokers from never-smokers based on the VBM analysis (details in the Results section below). Given the inconsistency in the literature with respect to the role of laterality of insula structure/function in nicotine addiction (Sutherland et al., 2013a; Zhang et al., 2011a), we also created bilateral anterior insula ROIs as 5×5×5 mm^3 cubes centered at voxel locations described by Cauda and colleagues (Cauda et al., 2011) (Fig. 2).

Physiological and other spurious sources of noise were estimated and regressed out using the anatomical CompCor method (aCompCor; (Behzadi et al., 2007)). Global signal regression, a widely used preprocessing method that mathematically introduces negative correlations (Murphy et al., 2009), was not used. The anatomical image for each participant was segmented into white matter (WM), grey matter, and cerebrospinal fluid (CSF) masks using SPM8. To minimize partial voluming with grey matter, the WM and CSF masks were eroded by one voxel, which resulted in substantially smaller masks than the original segmentations (Chai et al., 2012). The eroded WM and CSF masks were then used as noise regions of interest (ROI). Based on previous results (Chai et al., 2012), five principal components of the signals from WM and CSF noise ROIs were removed with regression. Previous results showed that a CompCor signals were considerably different from the global signal, as

regressing out higher order principal components of the global signal diminished both positive and negative correlations whereas regressing out aCompCor signals resulted in stronger anticorrelations and eliminated spurious correlations (Chai et al., 2012). A temporal band-pass filter of 0.009 Hz to 0.08 Hz was applied to the time series. Residual head motion parameters (3 rotation and 3 translation parameters, outliers identified by ART, plus another 6 parameters representing their first-order temporal derivatives) were regressed out.

First-level correlation maps were produced by extracting the residual blood oxygen level–dependent (BOLD) time course from each seed and computing Pearson's correlation coefficients between that time course and the time course of all other voxels. Correlation coefficients were converted to normally distributed z-scores using the Fisher transformation to allow for second-level General Linear Model analyses. For these analyses, we used the time courses for three seed regions: the VBM-based left anterior insula ROI and the bilateral anterior insula ROIs from (Cauda et al., 2011). To examine differences in connectivity between groups, first-level connectivity maps from each seed for each participant were entered into a group-level whole-brain Analysis of Covariance (ANCOVA) models with grey matter density values from the cluster that differentiated groups from the VBM analysis (left anterior insula extending into lateral prefrontal and temporal cortices) and total intracranial volume (TIV) as covariates in two independent ANCOVA models. We included regional grey matter density and TIV as covariates in these analyses in order to determine whether regional and/or global structural MRI differences account for significant variance in the models when functional connectivity is compared between groups. In all analyses, reported clusters survived a height threshold of uncorrected $p < .05$, and an extent threshold of FWE-corrected $p < .05$ at the cluster-level. Due to the modest sample size in each group, we also used data simulation to test the reliability of our results via bootstrapping (resampling with replacement) to test the reliability of any group differences in VBM or functional connectivity with the anterior insula (and adjacent structures) seeds (Supplementary Information).

Pearson product-moment correlations were calculated to test the association between structural and functional connectivity MRI data in all participants and with smoking behavior (severity of nicotine dependence via Fagerstrom Test of Nicotine Dependence, FTND; pack-years smoking; and number of cigarettes smoked per day) in smokers only. Analyses were performed with SPSS Version 21.0 (SPSS 21, IBM Corp. Released 2012. IBM SPSS Statistics for Mac, Version 21.0. Armonk, NY: IBM Corp.).

Results

Voxel-based morphometry (VBM)

Compared to never-smokers, smokers had significantly lower grey matter density in a cluster primarily in left anterior insula extending into inferior frontal gyrus and lateral temporal cortex (MNI coordinates: x = −34, y = 22, z = 14, cluster extent = 768; Fig. 1). There were no other group differences in grey matter density (all *ps* > .05).

Functional connectivity

Anterior insula connectivity—There was a group difference in right anterior insula correlation with a cluster consisting mostly of regions in right lateral prefrontal and temporal cortices, but also extending into ventromedial PFC and anterior cingulate cortex ($F(1,29) = 31.47$, cluster-level FWE-corrected $p < .001$; see Fig. 2, Table 2). In never-smokers, there was positive connectivity ($t(15) = 3.24$, cluster-level FWE-corrected $p = .006$) between these networks; however, these networks were anticorrelated in smokers ($t(15) = -3.10$, cluster-level FWE-corrected $p = .007$). The results were similar with or without VBM grey matter density included as a covariate in the model. There were no group differences in left anterior insula connectivity, either using the VBM-based ROI as a seed or the cubic ROI seed defined using the Cauda et al., 2011 criteria (all $ps > .05$).

Brain-smoking behavior correlations

Lower grey matter density in the lower left insula / inferior frontal cortex / lateral temporal cortex cluster from the VBM group difference was associated with a greater number of cigarettes smoked per day, ($r(14) = -.68$, $p = .004$; Fig. 3). There were no correlations between anterior insula network functional connectivity, VBM grey matter density, and smoking behavioral characteristics (all $ps > .1$).

Discussion

Previous studies have described both structural and functional abnormalities in brain networks involved in salience (anterior insula) and executive control (PFC) in cigarette smokers, which may partly explain pathological smoking behavior (see Goriounova and Mansvelder, 2012; Pan et al., 2013; Schuman-Olivier et al., 2014; Sutherland et al., 2012 for recent reviews). In this study, we measured MRI-based brain structure and functional connectivity in these regions / networks in acutely abstinent smokers and never-smokers and assessed whether brain structural differences could be used to identify functional differences and whether group differences in brain structure and functional connectivity correlated with smoking behavior. We found that smokers had lower grey matter density in a region comprising the left anterior insula and lateral PFC extending into lateral temporal cortex, and lower grey matter density in this region was associated with more cigarettes smoked per day. We observed group differences in functional connectivity, with never-smokers exhibiting a positive correlation and smokers exhibiting an anti-correlation between the right, but not left, anterior insula and right lateral PFC and temporal cortex extending into ventromedial PFC and anterior cingulate cortex.

Nicotine exposure, beginning in adolescence, alters synaptic structure and function in the insula and PFC, and this appears to be critical to the maintenance of ongoing smoking behavior and development of nicotine addiction (Goriounova and Mansvelder, 2012; Naqvi et al., 2014; Slotkin, 2002). In this study, we found lower grey matter density in smokers when compared to never-smokers, which is consistent with previous findings in smokers by some (Brody et al., 2004; Gallinat et al., 2006; Zhang et al., 2011b), but not others (Franklin et al., 2014; Morales et al., 2014; Zhang et al., 2011a). Inconsistencies in reported findings may be due to methodological issues such as cross-sectional designs with modest sample

sizes, and variations in definitions for smoking phenotypes (e.g., severity of nicotine dependence, psychiatric and medical co-morbidities, etc.), duration of smoking abstinence, MRI acquisition parameters and statistical methods for the analysis of the neuroimaging data. See (Franklin et al., 2014; Sutherland et al., 2012) for further discussion of these issues.

We also found group differences in functional connectivity between the right anterior insula and the right lateral PFC and temporal cortex extending into ventromedial PFC and anterior cingulate cortex with never smokers exhibiting a positive correlation and smokers exhibiting an anti-correlation. The anterior insula interfaces with the brain's reward system, including the ventral tegmental area in the midbrain, nucleus accumbens, amygdala, and ventromedial prefrontal cortex (including the medial orbitofrontal cortex) and appears to direct behavior based on the salience of internal and external cues (Chikama et al., 1997; Naqvi and Bechara, 2010; Postuma and Dagher, 2006). The anterior portion of the insula projects to the ventral medial aspect of the striatum, including the nucleus accumbens, and has been associated with reward, affective, and cognitive processes (Chikama et al., 1997; Sutherland et al., 2012). Altered structure and function of the anterior insula has a critical, yet complex role in addiction, with several theorized functions, including involvement in pathological incentive salience, tracking withdrawal-associated bodily states, dysexecutive control of addictive behavior, and orienting attention toward the internally-focused vs. externally-focused mental states (Naqvi and Bechara, 2010; Naqvi et al., 2014; Naqvi et al., 2007; Sutherland et al., 2012). The anterior insula has structural and functional connections with the lateral PFC, which is a critical cognitive control node that appears to regulate salience attribution to guide goal-directed behavior via higher-order executive functions (Goldstein and Volkow, 2011). Lateral PFC directs attention to the relevant information necessary to execute optimal goal-directed behavior (Sutherland et al., 2012). Although nicotine has cognitive enhancing properties when administered acutely (Hahn et al., 2007), chronic nicotine exposure leads to executive dysfunction, characterized by disrupted function and connections between brain regions involved in cognitive control, including lateral PFC (Goriounova and Mansvelder, 2012; Lerman et al., 2014; Sutherland et al., 2012). In the context of addiction, dysregulation of lateral PFC-reward network connectivity may account for the pathological salience attribution to nicotine and diminished voluntary control of drug-seeking behavior that characterizes this disorder (Goldstein and Volkow, 2011). Aberrant connectivity between anterior insula and lateral PFC may also explain the increased bias to immediate rewards at the expense of later rewards that can characterize those with addiction, and may explain, in part, the propensity for relapse (Clewett et al., 2014).

Abnormalities in brain structure, e.g. (Gallinat et al., 2006) and function e.g. (McClernon et al., 2008) in lateral temporal cortex have also been reported in relation to nicotine dependence. Together, lateral PFC and temporal cortex appear to function as a semantic cognition network with lateral temporal cortex involved in the semantic representation of information (Hodges et al., 1992) and lateral PFC involved in the manipulation and control of semantic information (Thompson-Schill et al., 1997; Whitney et al., 2011). These regions, especially lateral temporal cortex, also play a crucial role in emotion regulation (Buhle et al., 2013). It is not clear what role lateral temporal cortex may play in addiction and the data in

the present study cannot definitely resolve this question; however, deficits in lateral temporal cortex and PFC may contribute to the difficulty those with addiction have modifying pathological emotional responses that contribute to maintenance of addictive behaviors. In an independent sample, we found lower lateral temporal cortex activation when smokers tried to utilize emotional regulation strategies while viewing smoking images and negative correlation between LTC activation and self reported craving, (Stoeckel LE, 2014) suggesting that ineffective modulation of pathological thought processes in the context of internal and external cues may promote pathological substance use.

Finally, it is important to emphasize that the observed brain structure differences appear to be independent of the differences in functional connectivity (i.e., these two measures were not correlated). While grey matter density in left anterior insula was negatively correlated with cigarettes smoked per day, anticorrelations between right anterior insula and right lateral temporal cortex and PFC were not related to any of the smoking behavior data collected. It is not clear why there were disparate findings with respect to laterality differences in the volumetric and functional connectivity results. As mentioned previously, the literature on the laterality of the insula and the contribution to nicotine addiction has been somewhat inconsistent (Sutherland et al., 2013a; Zhang et al., 2011a). The functional significance of the functional connectivity results, which did not correlate with the smoking behavior data we collected in the current study, is also unclear at this time.

Limitations and caveats

In this study, we had a repetition time (TR) of 6 seconds, which is longer than most resting state fMRI studies; however, this was chosen so that we could acquire high-resolution whole-brain data (2mm isotropic voxels) without the use of parallel imaging. We believe this did not impact the results of our data for two reasons. First, a previous study by Van Dijk and colleagues found there was no significant difference in correlation strengths within and between resting-state functional networks when comparing TR = 2.5 and 5 seconds resting scans, and that correlation strengths stabilized with acquisition time of 5 min (TR = 5) (Van Dijk et al., 2010). Second, in the current and previous studies using the same acquisition parameters (TR = 6 s; (Chai et al., 2014; Redcay et al., 2013), we observed the typical resting-state network patterns observed in other studies in the literature.

While we detected significant group anatomical and functional connectivity differences, our power to detect individual and group differences between functional connectivity, grey matter density, and smoking behavior was limited by the constraints of our sample size. It is possible that the relatively less conservative voxel-wise approach we selected for the functional connectivity vs. volumetric analysis could have resulted in an increased chance of false positive findings for these analyses. We nevertheless employed a bootstrapping procedure to ensure outliers in our limited sample size did not influence our results. Finally, it is also possible that group differences between smokers and never smokers would have been greater if the period of smoking abstinence were increased.

Conclusions and Summary

In summary, we report lower grey matter density in anterior insula and adjacent brain regions (inferior frontal and lateral temporal cortex) in cigarette smokers compared to never smokers. Functional connectivity between the right insula and lateral PFC and temporal cortex extending into ventromedial PFC and anterior cingulate cortex was lower in in smokers compared to never-smokers, grey matter density in anterior insula was associated with an aspect of smoking behavior (daily cigarettes smoked). This study has two major contributions: (1) Structural MRI data was used to guide selection of ROIs for seed-based functional connectivity analyses. Based on the VBM results, our functional connectivity analysis was focused on the anterior insula. (2) This evidence from structural (volumetric) and functional connectivity MRI data adds further support to the hypothesis that the anterior insula plays an important role in nicotine addiction, in part, via disrupted connections with lateral PFC and temporal cortex extending to ventromedial PFC and anterior cingulate cortex, and lateral temporal cortex, an understudied region in the context of addiction and an important area of future research focus. In particular, it will be interesting to determine the role of lateral temporal cortex function in nicotine addiction, and whether the known roles for lateral temporal cortex (representation of semantic information, emotion regulation) are abnormal in individuals with nicotine addiction and/or whether exposure to nicotine and the constituents of cigarettes lead to disruptions in these functions, which may promote addictive behaviors and interfere with treatment success.

Supplementary Material

Refer to Web version on PubMed Central for supplementary material.

Acknowledgments

We wish to acknowledge Ms. Vanessa Calderon, Alice Coakley, Caroline Chan, Janani Raveendran, Satrajit Ghosh, Carlo de los Angeles, Jodi Gilman, Gretchen Reynolds, and Julia Stern for imaging study support, discussion of methods, assistance with manuscript preparation, and critical review of the manuscript. This research was carried out at the Athinoula A. Martinos Imaging Center at the McGovern Institute for Brain Research at the Massachusetts Institute of Technology. Finally, the study was supported by the Harvard Medical School Norman E. Zinberg Fellowship in Addiction Psychiatry Research (LES), a Brain & Behavior Research Foundation NARSAD Young Investigator Award (LES), the Charles A. King Trust (LES), NIH K23DA032612 (LES), and NIH K24 DA030443 (AEE).

Research grant support from Pfizer and Forum pharmaceuticals (AEE).

References

Avants BB, Tustison N, Song G. Advanced normalization tools (ANTS). Insight J. 2009

Behzadi Y, Restom K, Liau J, Liu TT. A component based noise correction method (CompCor) for BOLD and perfusion based fMRI. NeuroImage. 2007; 37:90–101. [PubMed: 17560126]

Breckel TP, Thiel CM, Giessing C. The efficiency of functional brain networks does not differ between smokers and non-smokers. Psychiatry research. 2013; 214:349–356. [PubMed: 24144504]

Brody AL, Mandelkern MA, Jarvik ME, Lee GS, Smith EC, Huang JC, Bota RG, Bartzokis G, London ED. Differences between smokers and nonsmokers in regional gray matter volumes and densities. Biological psychiatry. 2004; 55:77–84. [PubMed: 14706428]

Buhle JT, Silvers JA, Wager TD, Lopez R, Onyemekwu C, Kober H, Weber J, Ochsner KN. Cognitive Reappraisal of Emotion: A Meta-Analysis of Human Neuroimaging Studies. Cerebral cortex. 2013

Carrera E, Tononi G. Diaschisis: past, present, future. Brain : a journal of neurology. 2014; 137:2408–2422. [PubMed: 24871646]

Cauda F, D'Agata F, Sacco K, Duca S, Geminiani G, Vercelli A. Functional connectivity of the insula in the resting brain. Neuroimage. 2011; 55:8–23. [PubMed: 21111053]

Chai XJ, Castanon AN, Ongur D, Whitfield-Gabrieli S. Anticorrelations in resting state networks without global signal regression. NeuroImage. 2012; 59:1420–1428. [PubMed: 21889994]

Chai XJ, Ofen N, Gabrieli JD, Whitfield-Gabrieli S. Selective development of anticorrelated networks in the intrinsic functional organization of the human brain. Journal of cognitive neuroscience. 2014; 26:501–513. [PubMed: 24188367]

Chikama M, McFarland NR, Amaral DG, Haber SN. Insular Cortical Projections to Functional Regions of the Striatum Correlate with Cortical Cytoarchitectonic Organization in the Primate. The Journal of Neuroscience. 1997; 17:9686–9705. [PubMed: 9391023]

Clewett D, Luo S, Hsu E, Ainslie G, Mather M, Monterosso J. Increased functional coupling between the left fronto-parietal network and anterior insula predicts steeper delay discounting in smokers. Human brain mapping. 2014; 35:3774–3787. [PubMed: 24523255]

Cole DM, Beckmann CF, Long CJ, Matthews PM, Durcan MJ, Beaver JD. Nicotine replacement in abstinent smokers improves cognitive withdrawal symptoms with modulation of resting brain network dynamics. NeuroImage. 2010; 52:590–599. [PubMed: 20441798]

Craig AD. How do you feel--now? The anterior insula and human awareness. Nature reviews Neuroscience. 2009; 10:59–70.

Dale AM, Fischl B, Sereno MI. Cortical surface-based analysis. I. Segmentation and surface reconstruction. NeuroImage. 1999; 9:179–194. [PubMed: 9931268]

Das D, Cherbuin N, Anstey KJ, Sachdev PS, Easteal S. Lifetime cigarette smoking is associated with striatal volume measures. Addiction biology. 2012; 17:817–825. [PubMed: 21392170]

Doehrmann O, Ghosh SS, Polli FE, Reynolds GO, Horn F, Keshavan A, Triantafyllou C, Saygin ZM, Whitfield-Gabrieli S, Hofmann SG, Pollack M, Gabrieli JD. Predicting treatment response in social anxiety disorder from functional magnetic resonance imaging. JAMA psychiatry. 2013; 70:87–97. [PubMed: 22945462]

First, MB. Structured Clinical Interview for DSM-IV-TR Axis I Disorders: SCID-I. Biometrics Research Department, New York State Psychiatric Institutute; 2007.

Franklin TR, Wetherill RR, Jagannathan K, Johnson B, Mumma J, Hager N, Rao H, Childress AR. The effects of chronic cigarette smoking on gray matter volume: influence of sex. PloS one. 2014; 9:e104102. [PubMed: 25090480]

Gallinat J, Meisenzahl E, Jacobsen LK, Kalus P, Bierbrauer J, Kienast T, Witthaus H, Leopold K, Seifert F, Schubert F, Staedtgen M. Smoking and structural brain deficits: a volumetric MR investigation. The European journal of neuroscience. 2006; 24:1744–1750. [PubMed: 17004938]

Goldstein RZ, Volkow ND. Dysfunction of the prefrontal cortex in addiction: neuroimaging findings and clinical implications. Nat Rev Neurosci. 2011; 12:652–669. [PubMed: 22011681]

Goriounova NA, Mansvelder HD. Short- and long-term consequences of nicotine exposure during adolescence for prefrontal cortex neuronal network function. Cold Spring Harbor perspectives in medicine. 2012; 2:a012120. [PubMed: 22983224]

Hahn B, Ross TJ, Yang Y, Kim I, Huestis MA, Stein EA. Nicotine enhances visuospatial attention by deactivating areas of the resting brain default network. The Journal of neuroscience : the official journal of the Society for Neuroscience. 2007; 27:3477–3489. [PubMed: 17392464]

Hayasaka S, Nichols TE. Combining voxel intensity and cluster extent with permutation test framework. NeuroImage. 2004; 23:54–63. [PubMed: 15325352]

Hodges JR, Patterson K, Oxbury S, Funnell E. Semantic dementia. Progressive fluent aphasia with temporal lobe atrophy. Brain : a journal of neurology. 1992; 115(Pt 6):1783–1806. [PubMed: 1486461]

Hong LE, Gu H, Yang Y, Ross TJ, Salmeron BJ, Buchholz B, Thaker GK, Stein EA. Association of nicotine addiction and nicotine's actions with separate cingulate cortex functional circuits. Archives of general psychiatry. 2009; 66:431–441. [PubMed: 19349313]

Janes AC, Farmer S, Frederick B, Nickerson LD, Lukas SE. An increase in tobacco craving is associated with enhanced medial prefrontal cortex network coupling. PloS one. 2014; 9:e88228. [PubMed: 24505440]

Janes AC, Nickerson LD, Frederick Bde B, Kaufman MJ. Prefrontal and limbic resting state brain network functional connectivity differs between nicotine-dependent smokers and non-smoking controls. Drug and alcohol dependence. 2012; 125:252–259. [PubMed: 22459914]

Kalivas PW, Volkow ND. The neural basis of addiction: a pathology of motivation and choice. The American journal of psychiatry. 2005; 162:1403–1413. [PubMed: 16055761]

Kuhn S, Romanowski A, Schilling C, Mobascher A, Warbrick T, Winterer G, Gallinat J. Brain grey matter deficits in smokers: focus on the cerebellum. Brain structure & function. 2012; 217:517–522. [PubMed: 21909705]

Lerman C, Gu H, Loughead J, Ruparel K, Yang Y, Stein EA. Large-Scale Brain Network Coupling Predicts Acute Nicotine Abstinence Effects on Craving and Cognitive Function. JAMA psychiatry. 2014

Maldjian JA, Laurienti PJ, Burdette JH. Precentral gyrus discrepancy in electronic versions of the Talairach atlas. NeuroImage. 2004; 21:450–455. [PubMed: 14741682]

Maldjian JA, Laurienti PJ, Kraft RA, Burdette JH. An automated method for neuroanatomic and cytoarchitectonic atlas-based interrogation of fMRI data sets. NeuroImage. 2003; 19:1233–1239. [PubMed: 12880848]

McClernon FJ, Kozink RV, Rose JE. Individual differences in nicotine dependence, withdrawal symptoms, and sex predict transient fMRI-BOLD responses to smoking cues. Neuropsychopharmacology : official publication of the American College of Neuropsychopharmacology. 2008; 33:2148–2157. [PubMed: 17987060]

Menon V, Uddin LQ. Saliency, switching, attention and control: a network model of insula function. Brain structure & function. 2010; 214:655–667. [PubMed: 20512370]

Mihov Y, Hurlemann R. Altered amygdala function in nicotine addiction: insights from human neuroimaging studies. Neuropsychologia. 2012; 50:1719–1729. [PubMed: 22575084]

Morales AM, Ghahremani D, Kohno M, Hellemann GS, London ED. Cigarette Exposure, Dependence, and Craving Are Related to Insula Thickness in Young Adult Smokers. Neuropsychopharmacology : official publication of the American College of Neuropsychopharmacology. 2014

Murphy K, Birn RM, Handwerker DA, Jones TB, Bandettini PA. The impact of global signal regression on resting state correlations: are anti-correlated networks introduced? NeuroImage. 2009; 44:893–905. [PubMed: 18976716]

Naqvi NH, Bechara A. The insula and drug addiction: an interoceptive view of pleasure, urges, and decision-making. Brain structure & function. 2010; 214:435–450. [PubMed: 20512364]

Naqvi NH, Gaznick N, Tranel D, Bechara A. The insula: a critical neural substrate for craving and drug seeking under conflict and risk. Annals of the New York Academy of Sciences. 2014

Naqvi NH, Rudrauf D, Damasio H, Bechara A. Damage to the insula disrupts addiction to cigarette smoking. Science. 2007; 315:531–534. [PubMed: 17255515]

Pan P, Shi H, Zhong J, Xiao P, Shen Y, Wu L, Song Y, He G. Chronic smoking and brain gray matter changes: evidence from meta-analysis of voxel-based morphometry studies. Neurological sciences : official journal of the Italian Neurological Society and of the Italian Society of Clinical Neurophysiology. 2013; 34:813–817.

Perrachione TK, Ghosh SS. Optimized design and analysis of sparse-sampling FMRI experiments. Frontiers in neuroscience. 2013; 7

Postuma RB, Dagher A. Basal ganglia functional connectivity based on a meta-analysis of 126 positron emission tomography and functional magnetic resonance imaging publications. Cerebral cortex. 2006; 16:1508–1521. [PubMed: 16373457]

Redcay E, Moran JM, Mavros PL, Tager-Flusberg H, Gabrieli JD, Whitfield-Gabrieli S. Intrinsic functional network organization in high-functioning adolescents with autism spectrum disorder. Frontiers in human neuroscience. 2013; 7:573. [PubMed: 24062673]

Schuman-Olivier, Z.; Stoeckel, LE.; Weisz, E.; Evins, AE. Chapter Eleven - Smoking Effects in the Human Nervous System. In: Madras, B.; Kuhar, M., editors. The Effects of Drug Abuse on the Human Nervous System. Boston: Academic Press; 2014. p. 333-365.

Seeley WW, Menon V, Schatzberg AF, Keller J, Glover GH, Kenna H, Reiss AL, Greicius MD. Dissociable intrinsic connectivity networks for salience processing and executive control. The Journal of neuroscience : the official journal of the Society for Neuroscience. 2007; 27:2349–2356. [PubMed: 17329432]

Slotkin TA. Nicotine and the adolescent brain: insights from an animal model. Neurotoxicology and teratology. 2002; 24:369–384. [PubMed: 12009492]

Smith SM, Jenkinson M, Woolrich MW, Beckmann CF, Behrens TEJ, Johansen-Berg H, Bannister PR, De Luca M, Drobnjak I, Flitney DE. Advances in functional and structural MR image analysis and implementation as FSL. NeuroImage. 2004; 23:S208–S219. [PubMed: 15501092]

Stoeckel, LECV.; Curran, MT.; Evins, AE. Assessing Cognitive Regulation of Cigarette Craving to Identify Brain Regions for Real-Time fMRI Neurofeedback Training; 67th Annual Meeting of the MGH Scientific Advisory Committee; 2014.

Sutherland MT, Carroll AJ, Salmeron BJ, Ross TJ, Hong LE, Stein EA. Down-regulation of amygdala and insula functional circuits by varenicline and nicotine in abstinent cigarette smokers. Biological psychiatry. 2013a; 74:538–546. [PubMed: 23506999]

Sutherland MT, Carroll AJ, Salmeron BJ, Ross TJ, Stein EA. Insula's functional connectivity with ventromedial prefrontal cortex mediates the impact of trait alexithymia on state tobacco craving. Psychopharmacology. 2013b; 228:143–155. [PubMed: 23455594]

Sutherland MT, McHugh MJ, Pariyadath V, Stein EA. Resting state functional connectivity in addiction: Lessons learned and a road ahead. NeuroImage. 2012; 62:2281–2295. [PubMed: 22326834]

Thompson-Schill SL, D'Esposito M, Aguirre GK, Farah MJ. Role of left inferior prefrontal cortex in retrieval of semantic knowledge: a reevaluation. Proceedings of the National Academy of Sciences of the United States of America. 1997; 94:14792–14797. [PubMed: 9405692]

Van Dijk KRA, Hedden T, Venkataraman A, Evans KC, Lazar SW, Buckner RL. Intrinsic functional connectivity as a tool for human connectomics: theory, properties, and optimization. Journal of neurophysiology. 2010; 103:297. [PubMed: 19889849]

Watson D, Clark LA, Tellegen A. Development and validation of brief measures of positive and negative affect: the PANAS scales. Journal of personality and social psychology. 1988; 54:1063. [PubMed: 3397865]

Whitfield-Gabrieli S, Nieto-Castanon A. Conn: a functional connectivity toolbox for correlated and anticorrelated brain networks. Brain connectivity. 2012; 2:125–141. [PubMed: 22642651]

Whitney C, Kirk M, O'Sullivan J, Lambon Ralph MA, Jefferies E. The neural organization of semantic control: TMS evidence for a distributed network in left inferior frontal and posterior middle temporal gyrus. Cerebral cortex. 2011; 21:1066–1075. [PubMed: 20851853]

Zhang X, Salmeron BJ, Ross TJ, Geng X, Yang Y, Stein EA. Factors underlying prefrontal and insula structural alterations in smokers. NeuroImage. 2011a; 54:42–48. [PubMed: 20699124]

Zhang X, Salmeron BJ, Ross TJ, Gu H, Geng X, Yang Y, Stein EA. Anatomical differences and network characteristics underlying smoking cue reactivity. NeuroImage. 2011b; 54:131–141. [PubMed: 20688176]

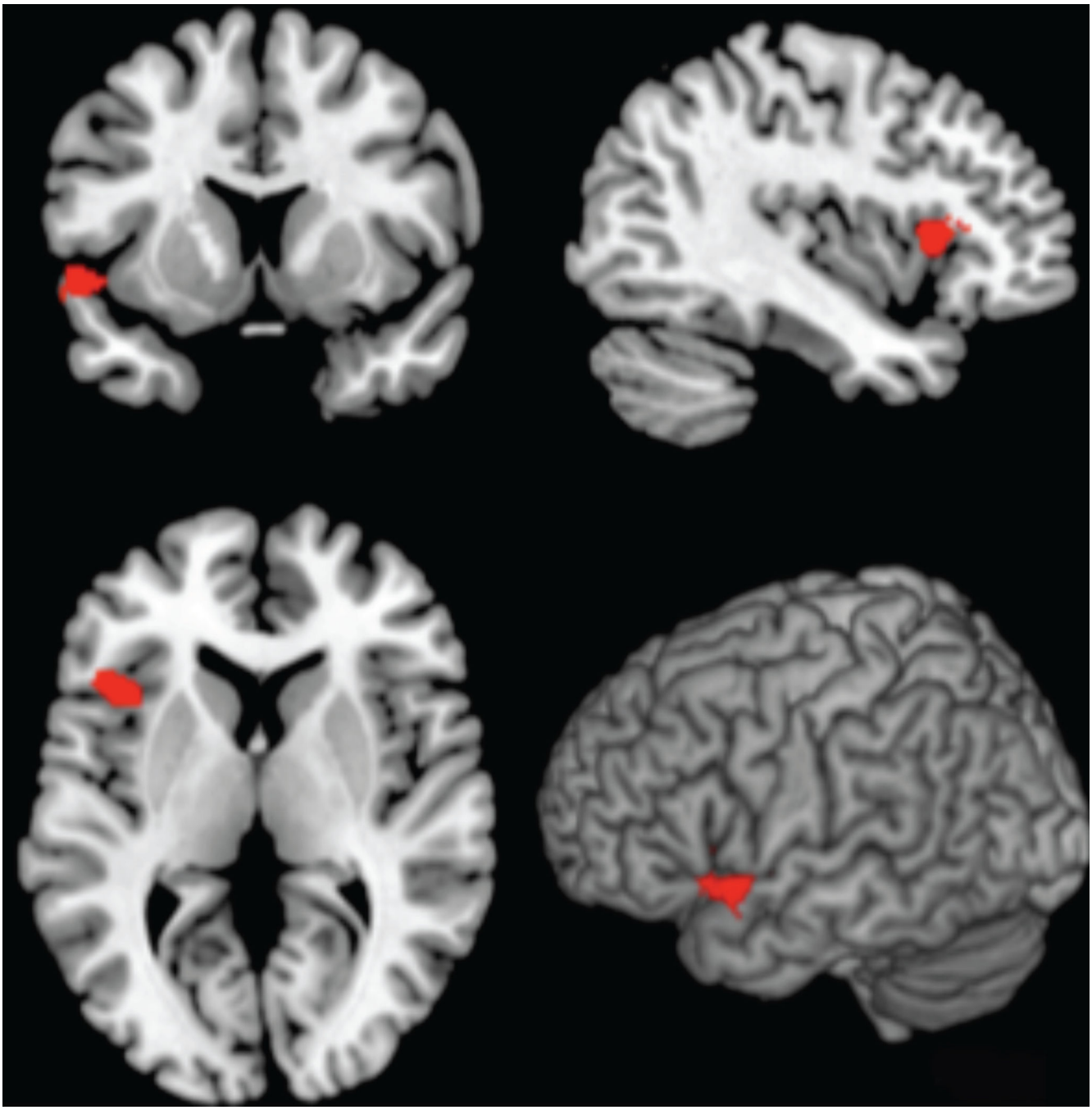

Fig. 1.

Lower grey matter density in left anterior insula, extending into inferior frontal gyrus and lateral temporal cortex (red) in smokers vs. controls (FWE-corrected, cluster level, $p < 0.05$, cluster extent = 768).

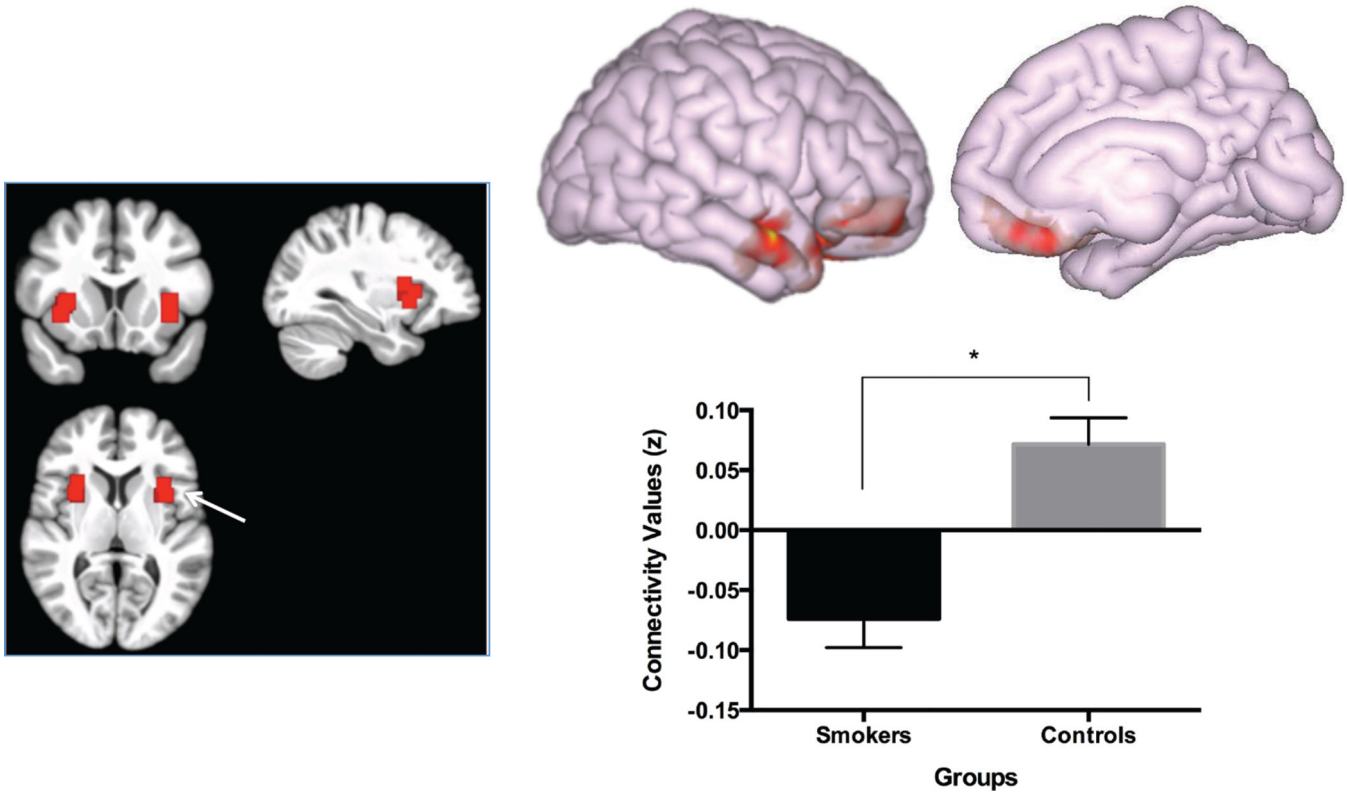

Fig. 2.

Left panel: bilateral anterior insula ROIs based on locations described by Cauda and colleagues (Cauda et al., 2011) overlaid on a template brain in MNI space created from the participant's high-resolution anatomical data. White arrow points to the right anterior insula seed. Right panel: top, medial and lateral view of the cluster showing different functional connectivity with the right anterior insula seed between smokers and never-smokers (cluster-level FWE-corrected $p < .001$); bottom, functional connectivity between the anterior insula and the cluster shown above in smokers and never-smokers. Bars represent the average connectivity (Fisher's z) in each group. Error bars represent standard errors.

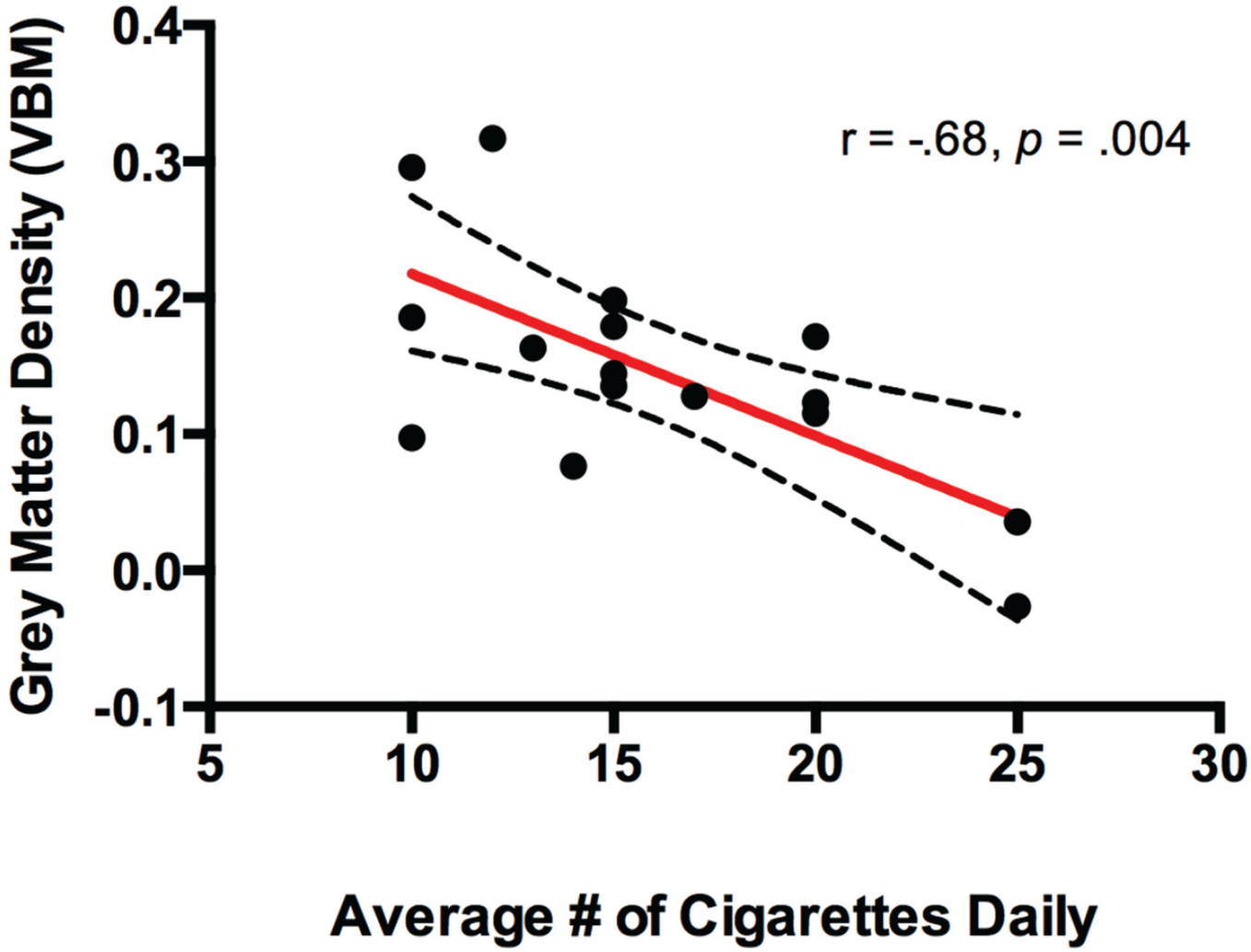

Fig. 3.

Scatterplot displaying significant negative correlation between VBM-based grey matter density (y-axis) and average number of cigarettes smoked daily (x-axis). Dotted lines represent 95% confidence intervals.

Table 1

Demographics& Smoking Characteristics in Study Participants

	Smokers n = 16	**Controls n = 16**	***p* value**
Age in years mean (SD)	37.94 (11.61)	34.19 (7.20)	n.s.
Sex (males / females)	12 / 4	11 / 5	n.s.
Education in years mean (SD)	14.44 (1.67)	15.25 (1.00)	n.s.
FTND mean (SD)	4.44 (2.16)	N/A	N/A
Pack-years of smoking mean (SD)	16.09 (12.17)	N/A	N/A
Cigarettes per day mean (SD)	16.00 (4.84)	N/A	N/A
Age of onset, daily smoking mean (SD)	17.97 (3.14)	N/A	N/A
Years of smoking mean (SD)	17.63 (10.49)	N/A	N/A

FTND = Fagerstrom Test of Nicotine Dependence; pack-years = # of packs of cigarettes smoked per day × # years as a smoker
n.s. = not significant
N/A = not applicable

Table 2

Lower connectivity in smokers vs. never-smokers in a network connected to the right anterior insula

Brain Region	BA[a]	# Vox[b]	% ROI[c]	Hem[d]	Cluster[e]	x[f]	y[f]	z[f]	*p*, FWE corrected[g]
OFC	11	431	18	R	2108	12	20	−32	< 0.001
IFC	47	247	13	R					
OFC	11	213	9	L					
Temporal Pole	38	104	6	R					
Anterior PFC	10	102	3	R					
Subgenual ACC	25	81	19	R					
Entorhinal Cortex	34	79	20	L					
Subgenual ACC	25	40	9	L					
Entorhinal Cortex	28	31	7	L					

[a] Brodmann area

[b] Number of voxels within each cluster

[c] Percentage of brain region included in each cluster

[d] Hemisphere: R, right, L, left

[e] Cluster size; number of contiguous voxels with $p < 0.05$

[f] x, y, and z coordinates in MNI space for peak voxel within the cluster

[g] Family wise error corrected at the cluster level

All listed brain regions are part of the same single cluster of contiguous voxels.

All results significant at $p < .05$, cluster-level family-wise error correction

OFC: orbitofrontal cortex; IFC: inferior frontal cortex; PFC: prefrontal cortex; ACC: anterior cingulate cortex